# Determinants of catalytic activity with the use of purified I, D and H subunits of the magnesium protoporphyrin IX chelatase from *Synechocystis* PCC6803[1]

Poul E. JENSEN[2], Lucien C. D. GIBSON and C. Neil HUNTER

Krebs Institute for Biomolecular Research and Robert Hill Institute for Photosynthesis, Department of Molecular Biology and Biotechnology, University of Sheffield, Sheffield S10 2TN, U.K.

The I, D and H subunits (ChlI, ChlD and ChlH respectively) of the magnesium protoporphyrin IX chelatase from *Synechocystis* have been purified to homogeneity as a result of the overexpression of the encoding genes in *Escherichia coli* and the production of large quantities of histidine-tagged proteins. These subunits have been used in an initial investigation of the biochemical and kinetic properties of the enzyme. The availability of pure ChlI, ChlD and ChlH has allowed us to estimate the relative concentrations of the three protein components required for optimal activity, and to investigate the dependence of chelatase activity on the concentrations of $MgCl_2$, ATP and protoporphyrin IX. It was found that, whereas ChlD and ChlH are likely to be monomeric, ChlI can aggregate in an ATP-dependent manner, changing from a dimeric to an octameric structure. Subunit titration assays suggest an optimal ratio of ChlI, ChlD and ChlH of 2:1:4 respectively. However, the dependence of chelatase activity on increasing concentrations of ChlI and ChlH with respect to ChlD suggests that these two subunits, at least *in vitro*, behave as substrates in their interaction with ChlD. Mg chelation could not be detected unless the $Mg^{2+}$ concentration exceeded the ATP concentration, suggesting at least two requirements for $Mg^{2+}$, one as a component of $MgATP^{2-}$, the other as the chelated metal. The steady-state kinetic parameters were determined from continuous assays; the $K_m$ values for protoporphyrin, $MgCl_2$ and ATP were 1.25 $\mu$M, 4.9 mM and 0.49 mM respectively. The rate dependence of $Mg^{2+}$ was clearly sigmoidal with a Hill coefficient of 3, suggesting positive co-operativity. Initiating the reaction by the addition of one of the substrates in these continuous assays resulted in a significant lag period of at least 10 min before the linear production of Mg protoporphyrin. This lag was significantly decreased by preincubating ChlI and ChlD with ATP and $MgCl_2$, and by mixing it with ChlH that had been preincubated with protoporphyrin IX, ATP and $MgCl_2$. This suggests not only a close $MgATP^{2-}$-dependent interaction between ChlI and ChlD but also an interaction between ChlH and the protoporphyrin substrate that also is stimulated by ATP and $MgCl_2$.

## INTRODUCTION

Magnesium protoporphyrin IX chelatase (Mg chelatase) catalyses the insertion of $Mg^{2+}$ into protoporphyrin IX, the first step unique to chlorophyll production. Mg chelatase and ferrochelatase, which catalyses the insertion of $Fe^{2+}$ into protoporphyrin IX, leading to the formation of haem, lie at the branch point of tetrapyrrole biosynthesis. So far Mg chelatase has not been subjected to detailed characterization with purified components, and the enzymology and regulation of this enzyme are of interest. It is now well established that Mg chelatase consists of three different subunits, I (38–42 kDa), D (60–74 kDa) and H (140–150 kDa), in (bacterio)chlorophyll *a*-producing prokaryotes [1–3] and also in higher plants [4–7]. In bacteriochlorophyll-producing organisms the three subunits are designated BchI, BchD and BchH whereas in chlorophyll-producing organisms they are designated ChlI, ChlD and ChlH. Thus Mg chelatase differs significantly from ferrochelatase, which is a single-subunit enzyme in all organisms studied so far [8,9]. Biochemically the two enzymes also differ: unlike ferrochelatase, Mg chelatase requires hydrolysable ATP besides the metal ion and porphyrin substrate, as shown by studies on chloroplast extracts [10]. In many respects Mg chelatase shows more similarities to the cobaltochelatase that inserts $Co^{2+}$ into hydrogenobyrinic acid *a*,*c*-diamide, a tetrapyrrolic precursor of vitamin $B_{12}$ [11]. This enzyme consists of a 140 kDa protein (CobN), which binds the tetrapyrrole, and a 450 kDa heteromeric protein composed of CobS and CobT, which are 38 and 80 kDa respectively and bind ATP [11]. Furthermore there is significant sequence similarity between CobN and the ChlH of Mg chelatase, although no significant similarities between ChlI/CobS and ChlD/CobT, apart from the respective molecular masses and an ATP-binding site consensus in the former protein pair.

The recent success in overexpressing the genes encoding the three Mg chelatase subunits from both *Rhodobacter sphaeroides* and *Synechocystis* PCC6803 in *Escherichia coli* and reconstitution of enzymic activity *in vitro* [1,2] provide excellent opportunities for the study of this enzyme. The mechanism of the reaction and the role of the individual protein subunits in the chelation reaction are not clear. Earlier work on chloroplast extracts suggested that magnesium chelation proceeds by a two-step reaction: an enzyme activation followed by a magnesium insertion step [10]. The activation step required the presence of hydrolysable ATP or adenosine 5′-[γ-thio]triphosphate (ATP[S]) and it was suggested that ATP could be required for oligomerization or as an activator [10]. The magnesium insertion step also seems to require ATP, although at a lower concentration than that needed for activation, and this cannot be replaced by ATP[S] [10]. Continuous assays with the *R. sphaeroides* Mg chelatase produced in *E. coli* have indicated that the BchI and BchD proteins are involved in the ATP-requiring activation step,

Abbreviations used: ATP[S], adenosine 5′-[γ-thio]triphosphate; DTT, dithiothreitol; Mg chelatase, magnesium protoporphyrin IX chelatase.

[1] C.N.H. would like to dedicate this paper to Professor Owen T.G. Jones on the occasion of his retirement.

[2] To whom correspondence should be addressed (e-mail P.E.Jensen@Sheffield.ac.uk.).

and it was proposed that ATP is required for the formation of a ternary complex between ATP and the BchI and BchD proteins [12]. The *R. sphaeroides* BchH protein has been suggested as the protoporphyrin IX carrier because the expression of BchH in *E. coli* cells results in the accumulation of large amounts of protoporphyrin [1], which stays bound to BchH during purification [12]. The BchI–BchD–ATP complex proposed above could then use $Mg^{2+}$ and the porphyrin bound to the BchH protein as the substrate for metal insertion, with the hydrolysis of ATP driving the reaction [12].

To test these proposals and suggestions it is necessary to have sufficient quantities of the three Mg chelatase proteins to conduct biochemical and enzymic studies of this important enzyme. This complex system will undoubtedly require detailed quantitative analysis but it is important to establish the basic properties of the system before further progress can be made. This paper presents the first results for the *Synechocystis* enzyme with the use of purified subunits. The basic properties of the chelation step have been characterized, including the association states of the individual subunits *in vitro* and the relative concentrations of protein components required for optimal activity. Furthermore continuous assays have been used to estimate the steady-state kinetic parameters and to investigate the subunit and substrate requirements during preincubation.

## EXPERIMENTAL

### Expression of recombinant proteins

The *Synechocystis chlI*, *chlD* and *chlH* genes were amplified by PCR with gene-specific primers, and cloned separately into the *Nde*I and *Bam*HI sites of expression vector pET14b [13], yielding plasmids pET14b-ChlI, pET14b-ChlD and pET14b-ChlH. The production of recombinant proteins was performed essentially as described in [2].

### Purification of the ChlI, ChlD and ChlH proteins

The cell pellets deriving from 500 ml cultures were thawed at room temperature and resuspended in 16 ml of cold binding buffer [5 mM imidazole/500 mM NaCl/20 mM Tris/HCl (pH 7.9)] and sonicated six times for 30 s on ice. Cell debris was spun down and the supernatants were processed on a $Ni^{2+}$-agarose affinity column (Novagen), in accordance with the manufacturer's instructions. The recombinant proteins were recovered by elution with imidazole buffer [500 mM imidazole/500 mM NaCl/20 mM Tris/HCl (pH 7.9)]. ChlI was dialysed into buffer A [50 mM Tricine/NaOH (pH 7.9)/300 mM glycerol/1 mM dithiothreitol (DTT)] and stored at −20 °C. ChlD and ChlH were further purified by anion-exchange chromatography with Q-Sepharose. ChlD was dialysed against buffer A containing 200 mM NaCl and loaded on a Q-Sepharose anion-exchange column (1 cm × 10 cm) equilibrated in the same buffer at a flow rate of 1 ml/min. The column was washed with 30 ml of buffer A containing 200 mM NaCl to remove unbound material, and bound proteins were eluted with a 95 ml linear gradient of 200–500 mM NaCl in buffer A. The ChlD-containing fractions were dialysed against buffer A. ChlH was purified in essentially the same way except that the proteins were eluted with a linear gradient of 100–700 mM NaCl.

### Gel filtration

Gel filtration was performed at 20 °C on a pre-packed Superose 6 HR column (1 cm × 30 cm) equilibrated with 50 mM Tricine/NaOH (pH 7.7)/100 mM NaCl/1 mM DTT at 0.4 ml/min. The column was calibrated with the following molecular mass markers: 2 mg/ml horse heart cytochrome *c* (12.4 kDa), 3 mg/ml bovine erythrocyte carbonic anhydrase (29 kDa), 10 mg/ml BSA (66 kDa), 5 mg/ml yeast alcohol dehydrogenase (150 kDa), 3 mg/ml sweet-potato $\beta$-amylase (200 kDa) and 2 mg/ml glutamate dehydrogenase (330 kDa). To determine the molecular masses of ChlI, ChlD and ChlH in solution, 200 $\mu$l aliquots of purified protein were loaded on the column. All three proteins were analysed in the above running buffer in the presence and in the absence of 4 mM $MgCl_2$, 2 mM ATP, and 4 mM $MgCl_2$ plus 2 mM ATP. Elution was followed by recording the absorbance at 280 nm. Peak fractions were analysed by enzyme assays.

### Mg chelatase assay

The standard assay was performed in 100 $\mu$l of buffer containing 50 mM Mops/NaOH, pH 7.7, 300 mM glycerol, 16 mM $MgCl_2$, 1 mM DTT, 5 mM ATP, 8 $\mu$M protoporphyrin IX and protein amounts as indicated in the figure legends. The assay mixtures were incubated for 30 min at 34 °C, stopped by the addition of 900 $\mu$l of acetone/water/32 % (w/v) ammonia (80:20:1, by vol.), and centrifuged at 15000 ***g*** for 5 min. A 1 ml sample of the aqueous phase was analysed on a SPEX FluoroLog spectrofluorimeter (SPEX Industries). The excitation wavelength was set to 420 nm and the emission spectrum was recorded between 550 and 650 nm. The fluorescence intensity response of Mg protoporphyrin IX was linear from 1 to 500 pmol when quantified by integration of the peak area caused by known amounts of authentic Mg protoporphyrin IX (Porphyrin Products, Logan, UT, U.S.A.). The amount of enzymically formed Mg protoporphyrin IX in each assay was quantified from this standard curve. The accumulation of product was linear for at least 30 min and the amount of product formed was on the linear part of the Mg protoporphyrin IX standard curve calculated for the fluorometric assay. Initial experiments showed that the temperature optimum was between 32–35 °C, that the pH optimum was between pH 7.5 and 7.9 and that the use of Mops instead of Tricine as a buffer during the assay resulted in a doubling in activity (results not shown). The optimal ATP concentration for the stopped assay was between 4 and 7 mM ATP in the presence of an excess of $MgCl_2$ (11 mM) (results not shown). It was found that 8 $\mu$M protoporphyrin IX gave optimal activity and inhibition was observed above the optimal concentration (results not shown).

Continuous assays were performed on a SPEX FluoroLog spectrofluorimeter with a fitted temperature-controlled cuvette holder set at 34 °C. The excitation wavelength was set to 420 nm and the emission wavelength was 596 nm. The assay volume was 1.0 ml and contained 300 mM glycerol, 50 mM Mops/NaOH, pH 7.7, 12 mM $MgCl_2$, 1 mM DTT, 1 mM ATP, 0.8 $\mu$M protoporphyrin IX and protein amounts as indicated in the legends to Figures 8, 9 and 10. A standard curve was made by diluting known amounts of authentic Mg protoporphyrin IX in assay buffer containing the same concentrations of ATP, $MgCl_2$ and chelatase subunits as the assays.

The apparent kinetic parameters were obtained by fitting the concentration dependence of the maximum reaction rate for each substrate, with the concentration of the other two substrates fixed close to saturation to the following equations:

$$v/[E]_t = V_{max}[S]/(K_m + [S]) \quad (1)$$

$$v/[E]_t = V[S]^h/(K_{0.5h} + [S]^h) \text{ (Hill equation)} \quad (2)$$

$$v/[E]_t = (V_{max*}[S])/(K_m + [S] + [S]^2/K_{si}) \text{ (simple inhibition)} \quad (3)$$

The kinetic parameters were estimated using the Marquardt–Levenberg curve-fitting algorithm (SigmaPlot; Jandel Scientific, Madera, CA, U.S.A.).

### Porphyrin solutions

Protoporphyrin IX (Sigma) was dissolved in dilute KOH and the pH adjusted to approx. 4 with HCl; the protoporphyrin IX was then extracted into ether. The ether phase was washed several times with 0.36 % (v/v) HCl before the porphyrin was extracted into 5 % (v/v) HCl. After adjustment of the pH to approx. 4 with NaOH the protoporphyrin IX was extracted back into ether and frozen overnight. On the next day, the protoporphyrin IX-containing ether was dried down and resuspended in 0.1 M $NH_4OH$ containing 1.5 % (v/v) Tween 80. Addition of the protoporphyrin IX in this solution to the assays was found to give significantly more Mg chelatase activity than adding it in DMSO (results not shown). The addition of up to 0.5 % (v/v) Tween 80 in the final assay was found to have no effect on enzyme activity. Mg protoporphyrin IX was resuspended in 0.1 M $NH_4OH$ containing 1.5 % (v/v) Tween 80 and diluted in acetone/water/32 % (v/v) ammonia (80:20:1, by vol.). Serial dilutions were performed and used to construct a standard curve. The concentration of protoporphyrin IX and Mg protoporphyrin IX was determined by taking $\epsilon_{554}$ as 13.5 $mM^{-1} \cdot cm^{-1}$ (2.7 M HCl) and $\epsilon_{419}$ as 308 $mM^{-1} \cdot cm^{-1}$ (ethanol) respectively.

### Other methods

SDS/PAGE was performed as described by Sambrook et al. [14]. Protein concentrations were determined with the Bio-Rad protein assay with BSA as standard. Calculation of the free $Mg^{2+}$ in solution with ATP was performed with WINMAXCHELATOR version 1.70 [15] and with the constants given by Brooks and Storey [16] adjusted for pH, temperature and ionic strength.

## RESULTS

### Purification of the overexpressed ChlI, ChlD and ChlH proteins

To fuse a hexahistidine ($His_6$) affinity tag to the proteins the *Synechocystis chlI*, *chlD* and *chlH* genes were cloned into pET14b. Comparison of the expression levels of the constructs in pET14b with those previously reported in pET3a or pET9a showed a similar level of each chelatase subunit and in assays the histidine-tagged proteins were as active as their non-tagged counterparts (results not shown). We therefore conclude that the N-terminal histidine tag has no apparent effect on the activity of the overexpressed ChlI, ChlD and ChlH proteins. All three proteins were purified on $Ni^{2+}$-agarose affinity columns directly from the supernatant after sonication of the *E. coli* cell pellet and removal of cell debris. Coomassie Blue-stained SDS/PAGE gels revealed that ChlI was pure after this step (Figure 1, lane 2), whereas the ChlD and ChlH preparations still contained other proteins (Figure 1, lanes 4 and 7). On the basis of the calculated pI values for ChlD and ChlH (4.9 and 4.8 respectively), both proteins were predicted to bind to an anion exchanger. The application of Q-Sepharose Fast Flow column chromatography and a NaCl gradient resulted in the elution of ChlD at pH 7.9 and 310–360 mM NaCl and of ChlH at pH 7.9 and 450–590 mM NaCl. This step removed the contaminating protein species from both the ChlD and ChlH preparations (Figure 1, lanes 5 and 8). In the ChlH preparation two minor contaminating proteins (85–90 and 50–55 kDa) could still be detected. These were most probably proteolytic degradation products of ChlH because their intensities always coincided with that of the ChlH protein when the fractions from the gradient elution were analysed with SDS/PAGE (results not shown). As observed during purification of the *R. sphaeroides* BchH protein [12], the *Synechocystis* ChlH protein exhibited a visible red colour after histidine tag purification, suggesting that this protein also binds protoporphyrin IX. However, after the subsequent ion-exchange chromatography step, protoporphyrin IX associated with ChlH could not be detected.

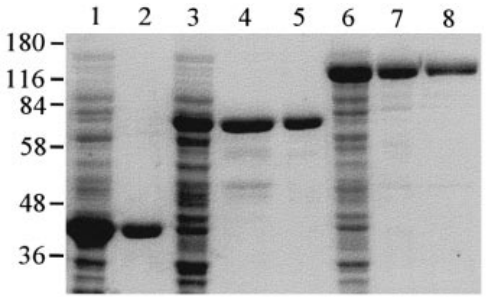


**Figure 1 SDS/PAGE demonstrating purification of proteins prepared from IPTG-induced *E. coli* strains containing the *chlI, chlD* and *chlH* genes**

Lanes 1, 3 and 6 show ChlI, ChlD and ChlH respectively before purification; lane 2, ChlI after HIS-TAG purification; lane 4 and 5, ChlD after histidine-tagging and Q-Sepharose purification respectively; lanes 7 and 8, ChlH after histidine-tagging and Q-Sepharose purification respectively. The positions of molecular mass markers are indicated at the left (in kDa).

**Table 1 Results of gel filtration**

Four different gel-filtration experiments were performed with the three purified Mg chelatase subunits: no addition, addition of 2 mM ATP and 4 mM $MgCl_2$, addition of 2 mM ATP, and addition of 4 mM $MgCl_2$ to the running buffer. Results are means ± S.D. for two or three replicates. Numbers without an S.D. are the results of a single determination.

| | | | Apparent molecular mass (kDa) | | | |
|---|---|---|---|---|---|---|
| Subunit | Concentration (mg/ml) | Addition ... | None | ATP + $MgCl_2$ | ATP | $MgCl_2$ |
| ChlI | 0.8 | | 81 ± 7 | 290 ± 6 | 76 | 93 ± 19 |
| | 2.0 | | 108 ± 11 | 290 ± 14 | 142 ± 7 | 194 |
| | 8.0 | | 208 | 278 | 165 | 208 |
| ChlD | 1.0–2.0 | | 128 ± 20 | 119 ± 14 | 120 ± 27 | 109 |
| ChlH | 1.4–3.2 | | 187 ± 12 | 208 | 208 | 192 ± 12 |

### Analytical gel filtration

The molecular masses of the native recombinant ChlI, ChlD and ChlH proteins were evaluated by size-exclusion chromatography on a Superose 6 column. The results are summarized in Table 1. From each column run with one Mg chelatase subunit the eluted fractions were tested for activity in assays with the other two subunits: the activity profile was superimposable on the elution peak.

The elution volume of the ChlI subunit was found to be concentration-dependent; at high ChlI concentrations the elution peak was asymmetrical with a shoulder towards lower elution volume (i.e. higher molecular mass species). Loading the column at the high protein concentration of 8 mg/ml results in a major elution peak corresponding to a molecular mass of 200 kDa, whereas more dilute samples yielded elution peaks corresponding to a molecular mass between 108 and 81 kDa. The molecular mass of ChlI is predicted to be 42.2 kDa (including the histidine tag) and was in good accordance with the mass seen on SDS/PAGE (Figure 1). At the most dilute concentration ChlI eluted as a protein with an apparent molecular mass of 81 kDa, suggesting a dimeric structure. Equilibrating

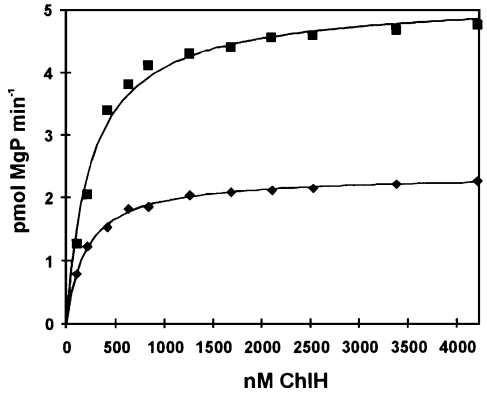


**Figure 2 Effect of varying the concentration of ChlH protein**

Various concentrations of ChlH were used with limiting concentrations of ChlD [1.31 nM (◆) and 2.62 nM (■)] and an excess of ChlI (570 nM). The results obtained are shown by the individual points and were used to estimate $K_m$ and $V_{max}$ by fitting to a rectangular hyperbola [eqn. (1)] with non-linear regression. These parameters were then used to simulate the curves shown. Abbreviation: MgP, magnesium protoporphyrin IX.

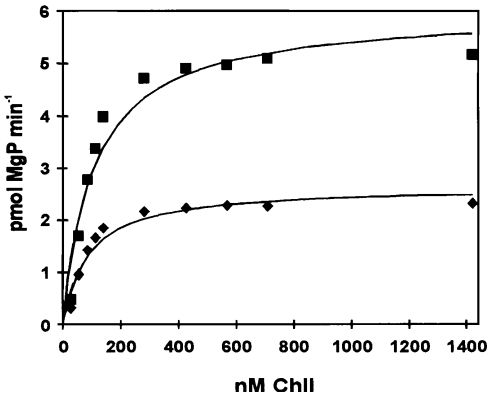


**Figure 3 Effect of varying the concentration of ChlI protein**

Various concentrations of ChlI were used with limiting concentrations of ChlD [1.31 nM (◆) and 2.62 nM (■)] and an excess of ChlH (1980 nM). The curves are simulations assuming that ChlI acts as a substrate as described in Figure 2. Abbreviation: MgP, magnesium protoporphyrin IX.

and running the column in buffer containing 2 mM ATP and 4 mM $MgCl_2$ resulted in consistent elution volumes giving an apparent molecular mass of $290 \pm 11$ kDa ($\pm$S.D.; $n = 5$). Furthermore the elution peak was symmetrical and the elution volume was independent of protein concentration. ATP or $MgCl_2$ alone in the running buffer did not have this effect on the elution volume. Thus $MgATP^{2-}$ induces the assembly of a ChlI complex containing eight ChlI monomers, at least *in vitro*.

The ChlD subunit was eluted as a single symmetrical peak showing an apparent molecular mass of $128 \pm 20$ kDa. The predicted monomeric molecular mass of ChlD is 76.2 kDa and is estimated to be approx. 80 kDa by SDS/PAGE (Figure 1). Thus the determination of the oligomeric state of ChlD in solution is ambiguous and we cannot exclude the possibility of an equilibrium between ChlD monomers and dimers, which could distort the elution characteristics of the subunit. The elution volume of ChlD was not affected by the presence of $MgCl_2$ and ATP.

The ChlH subunit was also eluted as a single symmetrical peak at an apparent molecular mass of $187 \pm 12$ kDa. The predicted molecular mass of ChlH is 151.2 kDa, which is in good agreement with the size determined from SDS/PAGE (Figure 1) and it therefore seems likely that ChlH is a monomer in solution. As for ChlD, the elution volume of the ChlH subunit was unaffected by the presence of $MgCl_2$ and ATP.

### Optimal amounts of the individual proteins

To estimate the subunit requirements a series of protein titration experiments were performed in which one of the subunits was in excess, one was present at a limiting concentration, and the concentration of the third was varied. The presence of excess concentrations of a given subunit was verified in experiments in which the concentration of the limiting subunit was doubled, resulting in a doubling of the activity.

The concentration of ChlH was varied, while keeping the concentration of the ChlD subunit constant at limiting concentrations in the presence of excess concentrations of ChlI (Figure 2). Inspection of the lower curve shows that saturation was reached at approx. 1.2 $\mu$M ChlH. At this point on the curve there were 900 molecules of ChlH present for every molecule of ChlD. It should be pointed out that there is a molar excess of protoporphyrin IX in this reaction and this curve is therefore assumed to provide information on the ChlH–ChlD interaction. Thus by regarding ChlD as the core catalytic subunit and ChlH as the substrate, and by assuming steady-state kinetic behaviour, the results were used to estimate $K_m$ and $V_{max}$ by non-linear regression. With 1.3 nM ChlD the apparent $V_{max}$ for ChlH was $13.8 \pm 0.12$ nmol/h per $\mu$g of ChlD and the $K_m$ was $0.20 \pm 0.009$ $\mu$M; for 2.6 nM ChlD the apparent $V_{max}$ for ChlH was $15.3 \pm 0.33$ nmol/h per $\mu$g of ChlD and the $K_m$ was $0.26 \pm 0.025$ $\mu$M. These parameters were then used to simulate a rectangular hyperbola for each data set. The simulations are displayed in Figure 2, and it is clear that in each case ChlH is behaving as the substrate in this reaction and obeying Michaelis–Menten kinetics.

In the next experiment ChlD was kept constant at limiting concentrations and the concentration of ChlI was varied in the presence of excess ChlH (Figure 3). From the lower curve and assuming saturation at 300 nM ChlI, there is an apparent ChlI-to-ChlD ratio of 200:1. As for the ChlH–ChlD interaction above, ChlD was regarded as the core catalytic subunit and ChlI as a substrate, and by assuming steady-state kinetic behaviour, the results were used to estimate $K_m$ and $V_{max}$. With 1.3 nM ChlD the apparent $V_{max}$ for ChlI was $15.8 \pm 0.72$ nmol/h per $\mu$g of ChlD and the $K_m$ was $0.085 \pm 0.017$ $\mu$M; with 2.6 nM ChlD the apparent $V_{max}$ for ChlH was $17.9 \pm 1.1$ nmol/h per $\mu$g of ChlD and the $K_m$ was $0.107 \pm 0.036$ $\mu$M. It should be noted that these values for the apparent $V_{max}$, which are approx. 16.8 nmol/h per $\mu$g of ChlD, are in agreement with those obtained with ChlH as the substrate, within experimental error, which demonstrates that in each experiment the correct concentration of excess substrate was chosen. The coincidence between the experimental data points and the simulated rectangular hyperbolic curves suggests that ChlI is behaving as a substrate in this reaction, and is conforming to the Michaelis–Menten relationship.

Figure 4(A) shows the results of varying the concentration of ChlD in the presence of limiting concentrations of ChlI and excess ChlH. With 23.7 nM ChlI an optimal rate is reached with approx. 13 nM ChlD, corresponding to a ChlI-to-ChlD ratio of 1.8:1; with 47.4 nM ChlI the optimal rate is reached with approx. 20 nM ChlD, giving a ChlI-to-ChlD ratio of 2.4:1. Thus a minimum ChlI-to-ChlD ratio of 2:1 is suggested, and it can be seen that increasing the concentration of ChlD above this ratio

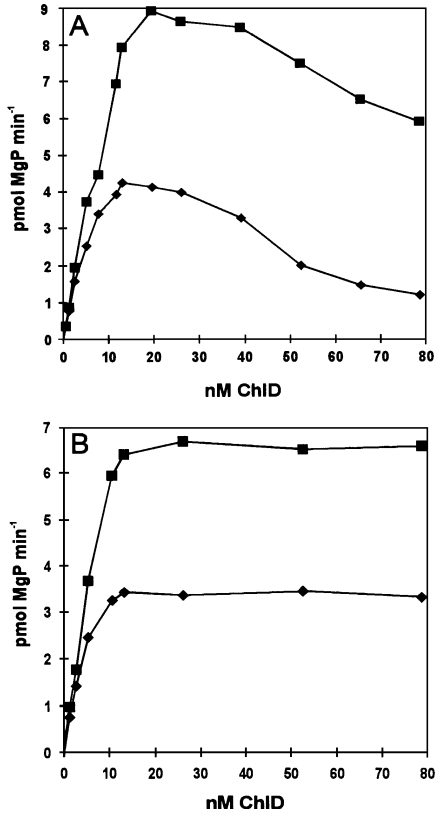


**Figure 4 Effect of varying the concentration of ChlD protein**

(**A**) Various concentrations of ChlD protein were used with limiting concentrations of ChlI [23.7 nM (◆) and 47.4 nM (■)] and an excess of ChlH (860 nM). (**B**) Various concentrations of ChlD protein were used with limiting concentrations of ChlH [212 nM (◆) and 424 nM (■)] and an excess of ChlI (570 nM). Abbreviation: MgP, magnesium protoporphyrin IX.

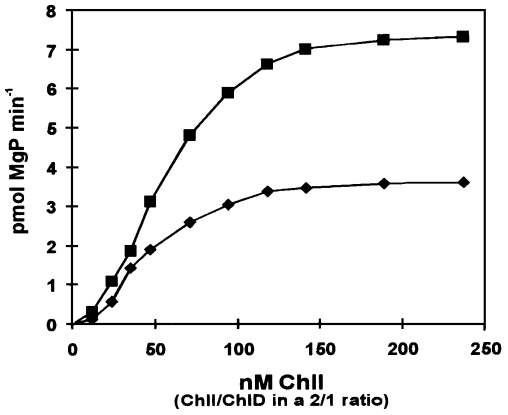


**Figure 5 Effect of varying concentration of (ChlI + ChlD)**

Various concentrations of ChlI plus ChlD, in a fixed 2:1 ratio, were assayed with limiting concentrations of ChlH [231 nM (◆) and 462 nM (■)]. Abbreviation: MgP, magnesium protoporphyrin IX.

results in inhibition. Owing to this inhibition arising from a ChlI-to-ChlD ratio greater than 2:1, it was not possible to perform the two experiments in which ChlD was present in excess; thus the ChlH-to-ChlI and ChlI-to-ChlH ratios could not be estimated.

Varying the concentration of ChlD in the presence of limiting concentrations of ChlH and excess ChlI yielded a ChlD-to-ChlH ratio of approx. 1:20 (Figure 4B).

The results in Figure 4(A) suggest a minimal ChlI-to-ChlD ratio of 2:1. By using this ratio the next experiment was performed to estimate the minimum ratio of ChlH to ChlI/ChlD. Increasing concentrations of ChlI and ChlD in a fixed 2:1 ratio were added to limiting concentrations of ChlH. With 230 nM ChlH, saturation was reached with approx. 120 nM ChlI/60 nM ChlD (Figure 5, lower curve), suggesting a minimal ratio of ChlI, ChlD and ChlH of 2:1:4 respectively. To ensure that the enzyme was limiting, 95 nM ChlI, 47 nM ChlD and 185 nM ChlH were used in all subsequent experiments.

From the $V_{max}$ estimates obtained from the results in Figures 2 and 3, where ChlD was limiting, a specific activity of 15.7 nmol of magnesium protoporphyrin IX/h per $\mu$g of ChlD was calculated. In a similar way we calculate a specific activity of 2.61 nmol of magnesium protoporphyrin IX/h per $\mu$g of ChlI from the results in Figure 4(A), where ChlI was limiting, and from Figure 4(B) and Figure 5, where ChlH was limiting, 0.06 nmol/h per $\mu$g of ChlH was obtained. This last value gives the most unfavourable view of the activity of the reconstituted Mg chelatase, and implies that of the three components, ChlH is the one most likely to limit the activity of the enzyme. We can calculate that in the assays in which ChlH was limiting (Figures 4B and 5), each molecule of ChlH was turning over approx. 4–5 times during a 30 min assay.

## Continuous assays: characterization of the lag period

Preliminary experiments, in which the three subunits and two of the substrates were preincubated at 34 °C for 10 min and the assay was initiated by adding the third substrate, consistently resulted in a 10 min lag period before the Mg protoporphyrin product accumulated at a linear rate. Continuous assays with the *R. sphaeroides* Mg chelatase subunits overproduced in *E. coli* had already indicated that BchI and BchD are involved in an ATP-requiring activation step that was necessary to overcome the lag period [12]. However, the situation with the *Synechocystis* Mg chelatase subunits seemed to be more complex because initiating the reaction by adding protoporphyrin to a preincubated mixture of ChlI, ChlD, ChlH, ATP and $MgCl_2$ still resulted in a lag, as well as suboptimal rates (Figure 6, compare traces 6 and 1). To characterize this lag period, a series of experiments were performed in which the overall chelation reaction was divided into two subreactions: one with ChlH and the other with ChlI/ChlD. In the first instance ChlI, ChlD, ATP and $MgCl_2$ were preincubated together for 10 min before mixing with ChlH. Preincubation of ChlH with ATP, $MgCl_2$ and protoporphyrin IX seemed to decrease the lag from 200 to 100 s, in comparison with ChlH preincubated with protoporphyrin IX alone (Figure 6, traces 1 and 4 respectively). Another series of experiments examined the effect of preincubating ChlI/ChlD/ATP/$MgCl_2$ with protoporphyrin (Figure 6, trace 5) or ChlH (Figure 6, trace 6). It is clear that neither of these preincubations resulted in the short lag seen in trace 1, and that neither protoporphyrin nor ChlH alone interacted with ChlI or ChlD in ways that affected the rate or shortened the lag. Therefore the only significant effect on the lag was seen when protoporphyrin was preincubated with ChlH, supporting the idea that one function of ChlH is to bind protoporphyrin before the chelation reaction.

The preincubation of ChlH with protoporphyrin, $MgCl_2$ and ATP had a marked effect on the maximum rate of chelation estimated from the linear part of each trace (Figure 6; compare traces 1 and 4). ChlH and protoporphyrin IX preincubated with

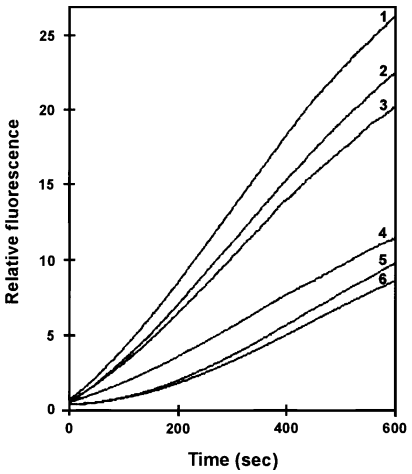


**Figure 6 Demonstration that preincubation of ChlH with protoporphyrin IX, ATP and $MgCl_2$ is necessary to reduce the lag in product formation and to reach maximal rate**

In traces 1–4 the preincubated ChlI/ChlD mixture was the same for all traces: 950 nM ChlI/470 nM ChlD/5 mM ATP/16 mM $MgCl_2$. This was mixed with 1850 nM ChlH preincubated with the following additions: trace 1, 8 $\mu$M protoporphyrin, 5 mM ATP and 16 mM $MgCl_2$; trace 2, 8 $\mu$M protoporphyrin, 5 mM ATP and 5 mM $MgCl_2$; trace 3, 8 $\mu$M protoporphyrin and 16 mM $MgCl_2$; trace 4, 8 $\mu$M protoporphyrin. For traces 5 and 6 either 8 $\mu$M protoporphyrin (trace 5) or 1852 nM ChlH (trace 6) was added to the ChlI/ChlD preincubation mixture. After preincubation, the incubation in trace 5 was mixed with 1852 nM ChlH that had been preincubated with 5 mM ATP and 16 mM $MgCl_2$; the incubation in trace 6 was mixed with protoporphyrin. All preincubations were for 10 min at 34 °C in a total volume of 100 $\mu$l. The final volume of all assays was adjusted to 1 ml with buffer of 34 °C and in all assays the final concentrations of protoporphyrin, ATP and $MgCl_2$ were 0.8 $\mu$M, 1 mM and 12 mM respectively and the final concentrations of ChlI, ChlD and ChlH were 95, 47 and 185 nM respectively.

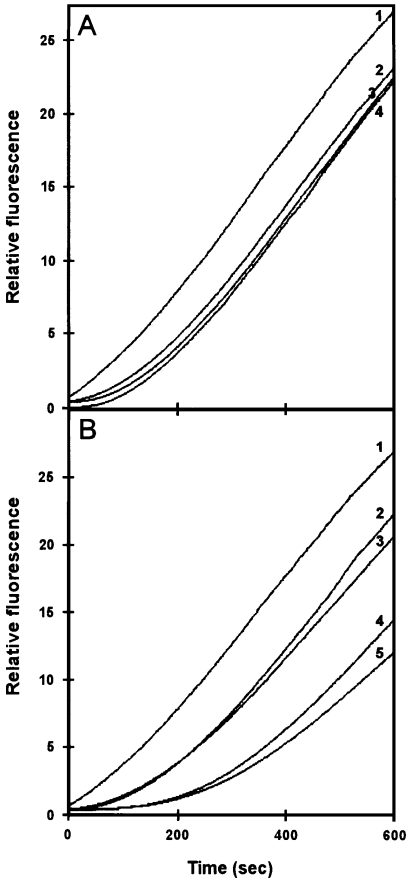


**Figure 7 Demonstration that preincubation of ChlI and ChlD with ATP and $MgCl_2$ is needed to overcome a lag in the linear rate of product formation**

(**A**) In these experiments the preincubated ChlH mixture was the same for all traces: 1850 nM ChlH/8 $\mu$M protoporphyrin/5 mM ATP/16 mM $MgCl_2$. This was mixed with 950 nM ChlI and 470 nM ChlD that had been preincubated with the following additions: trace 1, 5 mM ATP and 16 mM $MgCl_2$; trace 2, 11 mM $MgCl_2$; trace 3, 5 mM ATP and 5 mM $MgCl_2$; trace 4, no ATP and no $MgCl_2$. (**B**) In this series of experiments the effect of preincubating either ChlI or ChlD alone or with ChlH was investigated. Trace 1 is the same as in (**A**). For trace 2, ChlD was incubated with ChlH together with 8 $\mu$M protoporphyrin/5 mM ATP/16 mM $MgCl_2$. The reaction was started by adding ChlI. For trace 3, ChlD was preincubated with 5 mM ATP/16 mM $MgCl_2$ before being mixed with ChlH preincubated with 8 $\mu$M protoporphyrin/5 mM ATP/16 mM $MgCl_2$ and subsequently started by the addition of ChlI. For trace 4, ChlI was incubated with ChlH together with 8 $\mu$M protoporphyrin/5 mM ATP/16 mM $MgCl_2$ and the reaction was started by the addition of ChlD. For trace 5, ChlI was preincubated with 5 mM ATP/16 mM $MgCl_2$ before being mixed with ChlH preincubated with 8 $\mu$M protoporphyrin/5 mM ATP/16 mM $MgCl_2$ and subsequently started by the addition of ChlD. In all experiments the preincubation was in a volume of 100 $\mu$l and was conducted at 34 °C for 10 min. The final volume of the assay was adjusted to 1 ml with buffer at 34 °C and in all assays the final concentrations of the substrates and subunits were the same as in Figure 6.

either $MgCl_2$ or $MgATP^{2-}$, i.e. equimolar concentrations of ATP and $MgCl_2$, also caused a significant increase in the rate (Figure 6; compare traces 2 and 3 with trace 4). However, the highest rates, as seen in Figure 6 (trace 1), were repeatedly obtained when both $MgATP^{2-}$ and $MgCl_2$ were present during preincubation. This could indicate that besides protoporphyrin ChlH requires $MgATP^{2-}$ and $MgCl_2$ for proper function. A purely stabilizing effect of $MgATP^{2-}$ and $MgCl_2$ on ChlH is unlikely because preincubation of the three subunits with $MgATP^{2-}$ and $MgCl_2$, as indicated in Figure 6 (trace 6) followed by addition of protoporphyrin to start the reaction did not produce the maximal rate.

In the next series of experiments that part of the reaction involving ChlH was kept constant; thus ChlH was preincubated with protoporphyrin, ATP and $MgCl_2$ for 10 min before being mixed with different preincubations of ChlI and ChlD (Figure 7). These experiments confirmed that ChlI and ChlD are indeed involved in an ATP-dependent interaction (Figure 7; compare trace 1 with traces 2, 3 and 4). Neither $MgATP^{2-}$ nor $MgCl_2$ alone could reduce the lag. This strongly suggests that free $Mg^{2+}$ is required. In fact, $MgATP^{2-}$ or $MgCl_2$ alone in the ChlI plus ChlD preincubation resulted in a lag period of the same duration as preincubating ChlI and ChlD together without any nucleotide or $MgCl_2$ (Figure 7A; compare traces 2 and 3 with trace 4). Irrespective of the preincubation conditions used with ChlI plus ChlD, the final rate seemed to reach the same value. Preincubation of ChlI plus ChlD with ATP[S] followed by assay in the presence of ATP resulted in a trace similar to trace 2 in Figure 7(A), i.e. a lag period of the same duration as preincubating ChlI and ChlD together without any nucleotide or $MgCl_2$, followed by the same maximal rate as the control (results not shown). This examination of the lag period involving both ChlI and ChlD leads to the conclusion that ChlI and ChlD interact in an ATP-dependent manner that requires the presence of free $MgCl_2$.

Preincubation of ChlI or ChlD individually with $MgATP^{2-}$ and $MgCl_2$ was also tested and neither of these combinations decreased the duration of the lag (Figure 7B, traces 2 and 4). In fact, preincubation of ChlI with ATP and $MgCl_2$ for 10 min caused a marked increase in the lag period (Figure 7B, trace 5) and a similar effect was seen when ChlI was preincubated with

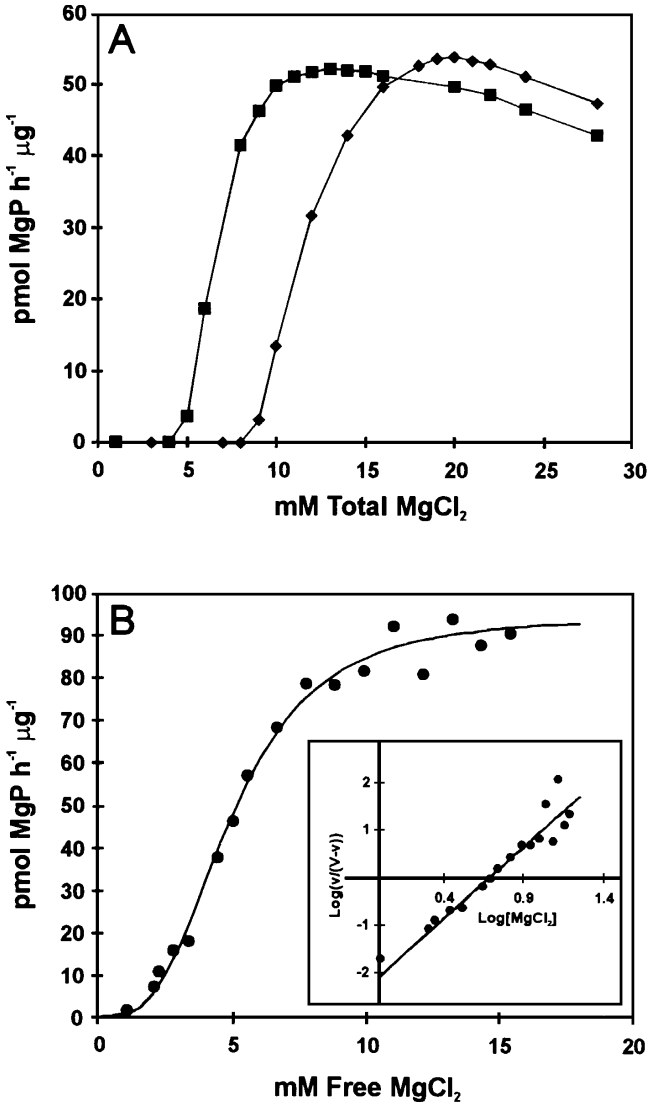


**Figure 8 Dependence on $MgCl_2$ concentration of the rate of Mg chelation catalysed by the reconstituted *Synechocystis* Mg chelatase**

(**A**) The stopped assay was used to investigate the requirement for free $Mg^{2+}$: no detectable Mg chelation takes place before the $MgCl_2$ concentration exceeds the ATP concentration. ChlI (95 nM), ChlD (47 nM) and ChlH (185 nM) were used in the standard assay with various concentrations of total $MgCl_2$ and with two different concentrations of ATP: 4 mM (■) and 8 mM (◆). (**B**) For the kinetic analysis the continuous assay was used to obtain the maximal rates. Reactions were initiated by mixing preincubated mixtures of ChlH/5 mM ATP/16 mM $MgCl_2$/8 $\mu$M protoporphyrin IX with a preincubated mixture containing ChlI, ChlD, 5 mM ATP and 16 mM $MgCl_2$. At final concentrations of free $MgCl_2$ below 2.2 mM the concentration of $MgCl_2$ in the preincubations was reduced and at final concentrations above 2.2 mM $MgCl_2$ the preincubations were mixed with warm buffer containing $MgCl_2$ to give the final concentrations as indicated. The final concentrations of ATP and protoporphyrin were 1 mM and 0.8 $\mu$M respectively. The results are shown by the individual points and were fitted to the Hill equation [eqn. (2)] by non-linear regression. The parameters obtained were then used to generate the curve. The inset shows $\log[v/(V-v)]$ plotted against $\log[MgCl_2]_{free}$; the parameters obtained for the Hill function were used to generate the line. The preincubations contained 950 nM ChlI, 470 nM ChlD and 1850 nM ChlH which were subsequently diluted 1:10 in the final 1 ml assay. Abbreviation: MgP, magnesium protoporphyrin IX.

ChlH, ATP, $MgCl_2$ and protoporphyrin (Figure 7B, trace 4). Therefore preincubation of ChlI with ATP and $MgCl_2$ in the absence of ChlD apparently converts ChlI into an unproductive

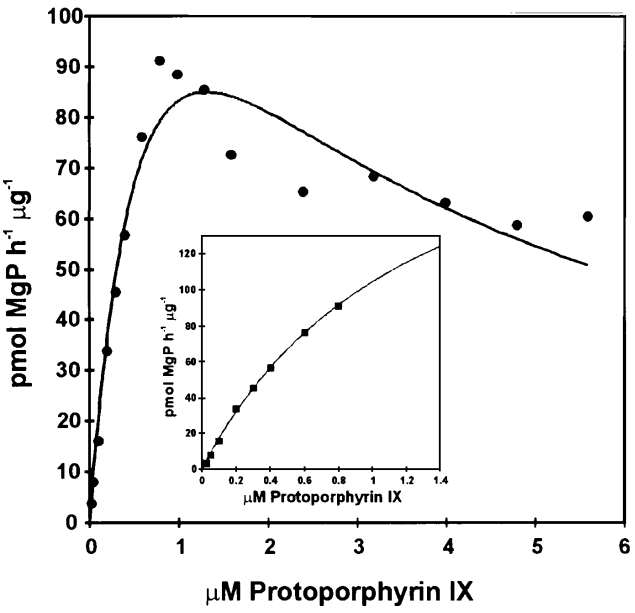


**Figure 9 Dependence on protoporphyrin IX concentration of the rate of Mg chelation catalysed by the reconstituted *Synechocystis* Mg chelatase**

Reactions were initiated by mixing a preincubated mixture containing ChlH, 5 mM ATP, 16 mM $MgCl_2$ and various concentrations of protoporphyrin IX with a preincubated mixture containing ChlI, ChlD, 5 mM ATP and 16 mM $MgCl_2$. At final concentrations of protoporphyrin below 0.8 $\mu$M the amount of protoporphyrin in the preincubations was decreased and at final concentrations above 0.8 $\mu$M the preincubations were mixed with warm buffer containing protoporphyrin to give the final concentrations as indicated. The final concentrations of ATP and $MgCl_2$ were 1 and 11 mM respectively. The results are shown by the individual points and were fitted to eqn. (3) by non-linear regression. The parameters obtained were then used to generate the curve. The inset shows the points up to 0.8 $\mu$M protoporphyrin; these were fitted to a rectangular hyperbola by using non-linear regression and the parameters obtained were used to generate the curve. The preincubations contained 950 nM ChlI, 470 nM ChlD and 1850 nM ChlH, which were subsequently diluted 1:10 in the final 1 ml assay. Abbreviation: MgP, magnesium protoporphyrin IX.

state, a process that seems to be reversible, because the rate eventually reaches that of the control.

## Measurements of steady-state kinetic parameters for the three substrates

Initial optimization of the $MgCl_2$ requirement for the Mg chelatase enzyme was performed with the stopped assay and revealed some interesting points. Mg chelatase activity could not be detected until the $MgCl_2$ concentration exceeded the ATP concentration, indicating that free $Mg^{2+}$ ions are needed for the formation of detectable amounts of products; it seems that the optimal $MgCl_2$ concentration is 10–12 mM above the ATP concentration (Figure 8A). Increasing the $MgCl_2$ concentrations above the optimal value resulted in a steady decrease in activity. This decrease could be due to either substrate inhibition, an effect of salt or precipitation of protein.

Maximum rates of magnesium chelation were determined with the continuous assay; the steady-state parameters for the reaction were determined from the concentration dependence of the maximum reaction rate for each substrate, with the concentration of the other two substrates fixed close to saturation. Each measurement was repeated two or three times. $MgCl_2$ concentration-dependent rates were obtained as described in the legend to Figure 8(B). The rate dependence of free $MgCl_2$ is clearly sigmoidal (Figure 8B) and fitting the results to the Hill function

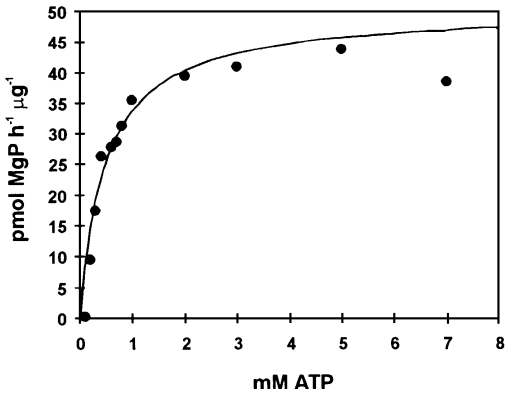


**Figure 10 Dependence on ATP concentration of the rate of the Mg chelation catalysed by the reconstituted *Synechocystis* Mg chelatase**

Reactions were initiated by adding warm buffer containing various concentrations of ATP to a mixture containing ChlI, ChlD, ChlH, $MgCl_2$ and protoporphyrin that had been preincubated for 5 min. The final concentrations of $MgCl_2$ and protoporphyrin were 11 mM and 0.8 $\mu$M respectively. In all three experiments the preincubations contained 950 nM ChlI, 470 nM ChlD and 1850 nM ChlH, which were subsequently diluted 1:10 in the final 1 ml assay. The results from 0.1 to 5 mM ATP were fitted to a rectangular hyperbola [eqn. (1)] by non-linear regression and the parameters obtained were used to generate the curve. Abbreviation: MgP, magnesium protoporphyrin IX.

reveals a satisfactory fit with the following apparent estimates of kinetic parameters for $MgCl_2$: $V_{max} = 95 \pm 3$ pmol/h per $\mu$g, $K_m = 4.9 \pm 0.2$ mM and $h = 3 \pm 0.3$. The $V_{max}$ obtained from the $Mg^{2+}$ dependence data is in agreement with the rate obtained with 800 nM protoporphyrin in Figure 9.

Figure 9 shows the result of varying the protoporphyrin concentration and there is a hyperbolic increase in the rate of Mg chelation with increasing protoporphyrin up to 0.8 $\mu$M. With protoporphyrin concentrations above 0.8 $\mu$M there is a reduction in the rate of Mg chelation to a constant level of activity. Fitting the results for up to 0.8 $\mu$M protoporphyrin (Figure 9, inset) to a rectangular hyperbola gave the following estimates of kinetic parameters for protoporphyrin: $V_{max} = 236 \pm 36$ pmol/h per $\mu$g and $K_m = 1.25 \pm 0.28$ $\mu$M. However, the maximum rate obtained with 0.8 $\mu$M protoporphyrin was only 92 pmol/h per $\mu$g. Attempts to fit the entire data set to a model with simple substrate inhibition [eqn. (3)] did not yield a satisfactory fit (Figure 9). One likely explanation for this is that protoporphyrin aggregates at high concentrations and is therefore not available to the enzyme. Therefore no further attempts were made to fit the data to an alternative model. Control experiments, in which protoporphyrin concentrations higher than 8 $\mu$M were added to the ChlH preincubation mixture, revealed the same level of inhibition as shown in Figure 9 and therefore the observed inhibition did not arise from the mixing conditions.

Owing to the interactions between the individual subunits and ATP the rate dependence on the ATP concentration was performed in a slightly different way. The three protein subunits were preincubated for 5 min with protoporphyrin and $MgCl_2$. The duration of the preincubation was less critical because no activation could take place in the absence of ATP. The reaction was initiated by mixing the preincubation with warm buffer containing various concentrations of $MgATP^{2-}$. In this way a constant excess of 11 mM free $MgCl_2$ above the ATP concentration was ensured. The rate increased in a hyperbolic manner with increasing ATP concentration until 5 mM and above this concentration some inhibition was seen (Figure 10). Fitting the data between 0.1 and 5.0 mM to a rectangular hyperbola gave the following apparent estimates of kinetic parameters for ATP: $V_{max} = 50 \pm 3$ pmol/h per $\mu$g and $K_m = 0.49 \pm 0.1$ mM. When this $V_{max}$ is compared with those obtained above for the $MgCl_2$ dependence, it is clear that the $V_{max}$ for ATP dependence reaches only approximately half of that obtained for $Mg^{2+}$ dependence; the steady-state estimates for ATP are therefore probably underestimated.

## DISCUSSION

### Provisional model

To our knowledge this is the first analysis of the biochemical and kinetic properties of a Mg chelatase from a chlorophyll *a*-synthesizing organism by using purified subunits. The purified subunits reconstitute to form a highly active enzyme but the complexity of the Mg chelatase enzyme precludes a full kinetic analysis. However, a conventional analysis assuming Michaelis–Menten kinetics for each substrate allows us a glimpse of the factors that determine the catalytic properties of Mg chelatase. A provisional model for Mg chelatase has recently been proposed by Walker and Willows [17]. In Scheme 1 a mechanistic version of the Mg chelatase cycle is presented, which in part is based on the model by Walker and Willows [17] and in part on the reaction cycle for nitrogenase described by Thorneley and Lowe [18] and Thorneley [19].

### The interaction between ChlI and ChlD

The results from the gel-filtration experiments indicate that $MgATP^{2-}$ has a marked effect on the aggregation behaviour of the ChlI subunit *in vitro*, converting it from a dimeric structure into an octamer. The existence of Type A and B ATP-binding motifs ($A/GX_4GKS/T$ and $H/R/KX_{5-8}OXOODE$, where O indicates hydrophobic residues) [20–22] in ChlI, is consistent with an effect of ATP and it seems that at least one function of ChlI is to bind $MgATP^{2-}$, an essential component of the chelation

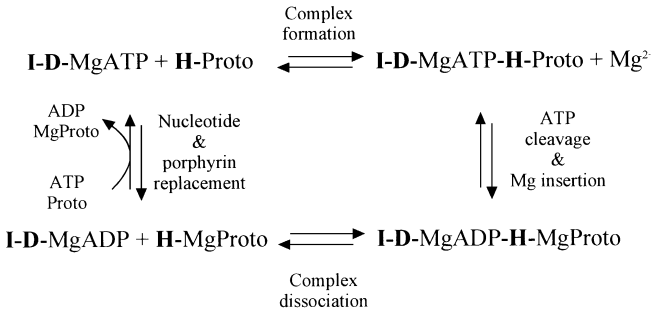


**Scheme 1 Model of the Mg chelatase cycle**

The ChlI and ChlD subunits interact with $MgATP^{2-}$ and a complex is probably formed (I–D–$MgATP^{2-}$). The ChlH subunit with bound protoporphyrin (Proto) reacts with this ChlI–ChlD–$MgATP^{2-}$ complex; a short-lived complex consisting of all three subunits and at least two of the substrates is formed (complex formation). Next, $Mg^{2+}$ is inserted into protoporphyrin IX with the concomitant hydrolysis of ATP, resulting in another, probably short-lived, complex consisting of ChlI, ChlD, ChlH, MgADP and Mg protoporphyrin (MgProto). This dissociates into ChlI–ChlD–MgADP and ChlH–MgProto, which then can be recharged with $MgATP^{2-}$ and protoporphyrin and participate in a new reaction cycle.

reaction. However, the continuous assays demonstrate that the ChlI/$MgATP^{2-}$ preincubation caused a marked increase in the lag period before a linear rate of product formation was observed, which suggests that a ChlI–$MgATP^{2-}$ complex is unfavourable for the chelation reaction. In the presence of ChlD and ChlI, ATP and $MgCl_2$ are absolutely required in order to overcome the lag and, as indicated in Scheme 1, a $MgATP^{2-}$-dependent interaction between the ChlI and ChlD subunits before interaction with the ChlH subunit is suggested. In nitrogenase, $MgATP^{2-}$ binding induces protein conformational changes that favour the formation of the Fe protein–MoFe protein complex [23,24], and function of the subsequent hydrolysis of $MgATP^{2-}$ in this case has been suggested to be to induce protein conformational changes that would be coupled to protein–protein dissociation [25]. It remains to be established whether a similar mechanism is true for Mg chelatase.

The results of the ChlI/ChlD subunit titration show that, at least *in vitro*, there is no practical limit to the ChlI-to-ChlD ratio (Figure 3), although it is likely that the ratio determined (approx. 200:1) is not remotely approached *in vivo*. The converse experiment, in which the concentration of ChlD is increased, showed that when the ChlD-to-ChlI ratio exceeds 1:2, inhibition of the reaction occurs (Figure 4A); it is tempting to speculate that the ChlI–ChlD–$MgATP^{2-}$ complex indicated in Scheme 1 has a 1:1 stoichiometry of $ChlI_2$ to ChlD.

The *R. sphaeroides* BchD purified from an *E. coli* overexpression strain has been reported to be polymeric with a molecular mass of approx. 550 kDa [12]. However, the gel-filtration experiments reported here with ChlD under different conditions showed that ChlD is likely to be monomeric, or possibly dimeric and although the gel filtration results for ChlD are ambiguous in this respect, there are no indications of aggregation of ChlD into an oligomer. It is therefore unlikely that the ChlD dissociates from a ChlD aggregate as proposed in the model by Walker and Willows [17].

In Scheme 1 we assume that the inserted $Mg^{2+}$ comes from the pool of free $Mg^{2+}$ and not from the $MgATP^{2-}$ complex. One possible role of ChlD is to bind the $Mg^{2+}$ ion transiently before insertion into protoporphyrin IX. There is a region of negatively charged residues in ChlD in which 19 out of 40 residues are either Asp or Glu and which is flanked by proline-rich regions [2]. Predictions of secondary structure suggest that this acidic region is organized into an $\alpha$-helix with one side lined with these acidic residues. In other $Mg^{2+}$-requiring enzymes large numbers of carboxylic ligands have been reported to form a typical $Mg^{2+}$-binding domain [26]. Thus the cluster of negative charges might function as a $Mg^{2+}$-binding pocket; such an apparent abundance of negative charges might be necessary to encourage the elimination of the hydration shell around the $Mg^{2+}$ ion, which is a precondition for the subsequent insertion into protoporphyrin IX [27]. The proline-rich regions are likely to be flanking segments of contact sites for subunit interactions [28]. The model in Scheme 1 therefore differs from the model proposed by Walker and Willows, in which the $Mg^{2+}$ is thought to bind to the ChlH subunit before insertion. These propositions will be tested in future experiments.

### Confirmation that ChlH interacts with protoporphyrin

During histidine-tag purification of ChlH, it was noted that ChlH-containing fractions exhibited a visible red colour most probably contributed by protoporphyrin sequestered during overproduction of this protein in *E. coli*. During the subsequent anion-exchange purification step the protoporphyrin was lost. This is quite different from the observations made during purification of the *R. sphaeroides* BchH, in which a significant amount of protoporphyrin remained bound during three chromatographic steps [12]. This could suggest that ChlH has less affinity for protoporphyrin than BchH or that it needs additional factors for proper binding. The continuous assays performed with ChlH suggest that it needs to interact with protoporphyrin to decrease the lag before the onset of chelation. Furthermore this ChlH–protoporphyrin interaction was greatly stimulated by $MgCl_2$ or $MgATP^{2-}$, with the strongest stimulation when both $MgATP^{2-}$ and an excess of $MgCl_2$ were present. However, preincubation of ChlH with ATP and $MgCl_2$ but no protoporphyrin was ineffective in decreasing the extent of the lag period, which makes a stabilizing effect of ATP and $MgCl_2$ less likely than a specific interaction with protoporphyrin. Thus, besides supporting the notion that ChlH interacts with protoporphyrin before chelation, the continuous assays also suggest that ChlH requires both $MgATP^{2-}$ and $MgCl_2$ in order to interact properly with protoporphyrin.

### Interaction between ChlH and ChlD

As discussed above, it is likely that the ChlH subunit binds protoporphyrin IX before $Mg^{2+}$ insertion and, as indicated in Scheme 1, it seems that at least one role of ChlH is to act as a substrate carrier. In support of this, we observe a relatively high ChlH-to-ChlD ratio in the subunit titration (Figure 2), as well as noting that the relationship between these proteins in terms of Mg chelation is well described by the Michaelis–Menten equation. The requirement for the ChlH subunit might be twofold: first, as a method of sequestering protoporphyrin IX to prevent the insertion of $Fe^{2+}$ by ferrochelatase, as proposed for the *Arabidopsis* CHL H protein [29], and secondly, as a way of presenting protoporphyrin to the ChlI–ChlD complex to fulfil a precise structural arrangement with regard to this complex and thereby being part of the active site (Scheme 1, complex formation).

A Mg chelatase complex has never been purified from any organism. Most work so far suggests that the Mg chelatase subunits in both *R. sphaeroides* and higher-plant chloroplasts exist separately from each other and activity could be reconstituted only by combining different fractions [5,6,30]. This could suggest that any interactions holding the subunits in a putative Mg chelatase complex together are weak or that the complex is short-lived. This might explain the observations in Figure 2, where there is no apparent limit to the amount of ChlH that can be added to the reaction, suggesting that replacement of ChlH in the putative complex with a new ChlH subunit with bound substrate is more favourable than recharging the subunits with substrate. The situation with ChlI is more subtle because the continuous assays indicate that ChlI and ChlD are both needed for an ATP-dependent activation process. Thus the function of ChlI could be to participate in this activation, which is also in accordance with the observed behaviour of ChlI in the experiment where increasing concentrations of ChlI are added to the reaction (Figure 3). However, work with the *R. sphaeroides* Mg chelatase subunits suggests that both the ChlI and ChlD subunits are needed to complete the catalytic cycle because separation of the two subunits after activation resulted in loss of activity [12].

### Kinetics of the Mg chelation reaction

The $K_m$ values obtained for ATP and $MgCl_2$ were 0.49 and 4.9 mM respectively, 3-fold the corresponding values reported for the *R. sphaeroides* Mg chelatase [12]. The $K_m$ for protoporphyrin was estimated to be 1.25 $\mu$M, whereas the value for

the *R. sphaeroides* system is 0.36 $\mu$M [12] and the recently published estimate obtained with partly purified Mg chelatase from developing pea leaves is 0.008–0.014 $\mu$M [6]. Both *R. sphaeroides* and plants need to channel large amounts of protoporphyrin to the chlorophyll pathway. In contrast, cyanobacteria synthesize large amounts of haem via ferrochelatase, because haem is an intermediate in the biosynthesis of the chromophore of phycobiliprotein, the major light-harvesting structure in these organisms [31]. The differences in $K_m$ values for Mg chelatases from the different sources therefore probably reflect different physiological needs, and the kinetics reported here provides at least one of the explanations for major allocations in the flux down these pathways, at the molecular level.

The sigmoidal shape of the $MgCl_2$ dependence curve with an estimated Hill coefficient of 3 suggests positive co-operativity. With partly purified Mg chelatase from developing pea leaves, Guo et al. [6] also find that the $Mg^{2+}$ concentration curve is strongly sigmoidal and report an apparent $K_m$ of 14.3 mM. The finding that the $MgCl_2$ concentration has to exceed the ATP concentration before chelation takes place confirms that $MgATP^{2-}$ is the active nucleotide species used during chelation, as suggested by Richter and Rienits [32], and thereby indicates one obvious role for $Mg^{2+}$. It also suggests that the enzyme requires free $Mg^{2+}$ ions for activity. The effect of $Mg^{2+}$ on co-operativity must be applied to parts of the reaction other than those involving a complex with ATP. An obvious role for $Mg^{2+}$, besides that of inserting into protoporphyrin, is to enhance and maintain subunit interactions, and the observed requirement for $Mg^{2+}$ in excess of the ATP concentration in the continuous assays with ChlI and ChlD (Figure 7A) is consistent with this purpose.

The kinetics obtained by varying the ATP concentration was subject to a significant limitation, in that the chelation reaction was initiated by the addition of ATP, thus depriving the subunits of the opportunity to interact with, and to be activated by, ATP. Accordingly we observed a relatively low $V_{max}$ in these assays. This highlights the central importance of ATP for the formation of a putative catalytic complex. The requirement for ATP must be at least threefold: (1) for the ChlI–ChlD interaction as indicated from the continuous assays (Figure 7A), (2) for the interaction with ChlH to ensure maximal rate (Figure 6), and (3) as energy source during metal insertion. It is therefore surprising that the ATP dependence curve is simply hyperbolic, in contrast with the multiple roles above for $Mg^{2+}$ and the consequent deviation from a simple hyperbolic curve. ATP could very well be the main regulator of Mg chelation because its availability and the interaction with $MgCl_2$ are key factors in the function of the enzyme.

Overall, the chelation of $Mg^{2+}$ seems to be a difficult reaction relative to the chelation of $Fe^{2+}$ because the insertion of $Mg^{2+}$ requires three proteins and ATP in contrast with ferrochelatase. We have already noted the contrast in affinities of the Mg chelatase enzymes for protoporphyrin, the shared substrate. In ferrochelatases from pea and *R. sphaeroides*, the $K_m$ values for protoporphyrin were reported to be 2.4 and 18 $\mu$M respectively [33,34]; in contrast, $K_m$ values of 0.36, 1.25 and 0.008–0.014 $\mu$M were obtained for Mg chelatase of *R. sphaeroides* [12], *Synechocystis* (the present study) and the pea system [6] respectively. These differences might have some important implications for the regulation of flux down the tetrapyrrole biosynthetic pathway, because this contrast in $K_m$ for a shared substrate would then be reflected in a dominance of the $Mg^{2+}$ branch over the $Fe^{2+}$ insertion. In many photosynthetic organisms, $Mg^{2+}$ chelation is a process that must prevail over $Fe^{2+}$ chelation. This necessity has driven the formation of a complex, multisubunit, multistep enzyme mechanism, which we will now be able to study at a detailed molecular level.

We thank Dr. Giles E. M. Martin and Professor Roger N. F. Thorneley for helpful discussions. This work was supported by grants from the Danish Agricultural and Veterinary Research Council (9400619) (P.E.J.) and from the Biotechnology and Biological Sciences Research Council, U.K. (C.N.H.).

## REFERENCES

1 Gibson, L. C. D., Willows, R. D., Kannangara, C. G., von Wettstein, D. and Hunter, C. N. (1995) Proc. Natl. Acad. Sci. U.S.A. **92**, 1941–1944
2 Jensen, P. E., Gibson, L. C. D., Henningsen, K. W. and Hunter, C. N. (1996) J. Biol. Chem. **271**, 16662–16667
3 Petersen, B. L., Jensen, P. E., Gibson, L. C. D., Stummann, B. M., Hunter, C. N. and Henningsen, K. W. (1997) J. Bacteriol. **180**, 699–704
4 Jensen, P. E., Willows, R. D., Petersen, B. L., Vothknecht, U. C., Stummann, B. M., Kannangara, C. G., von Wettstein, D. and Henningsen, K. W. (1996) Mol. Gen. Genet. **250**, 383–394
5 Kannangara, C. G., Vothknecht, U. C., Hansson, M. and von Wettstein, D. (1997) Mol. Gen. Genet. **254**, 85–92
6 Guo, R., Lou, M. and Weinstein, J. D. (1998) Plant Physiol. **116**, 605–615
7 Papenbrock, J., Grafe, S., Kruse, E., Hanel, F. and Grimm, B. (1997) Plant J. **12**, 981–990
8 Dailey, H. A. (1990) in Biosynthesis of Haem and Chlorophylls (Dailey, H. A., ed.), pp. 123–162, McGraw-Hill, New York
9 Hansson, M. and Hederstedt, L. (1994) Eur. J. Biochem. **220**, 201–208
10 Walker, C. J. and Weinstein, J. D. (1994) Biochem. J. **299**, 277–284
11 Debussche, L., Couder, M., Thibaut, D., Cameron, B., Crouzet, J. and Blanche, F. (1992) J. Bacteriol. **174**, 7445–7451
12 Willows, R. D., Gibson, L. C. D., Kannangara, C. G., Hunter, C. N. and von Wettstein, D. (1996) Eur. J. Biochem. **235**, 438–443
13 Rosenberg, A. H., Lade, B. N., Chui, D.-S., Lin, S.-W., Dunn, J. J. and Studier, F. W. (1987) Gene **56**, 125–135
14 Sambrook, J., Fritsch, E. F. and Maniatis, T. (1989) Molecular Cloning: A Laboratory Manual, 2nd edn., Cold Spring Harbor Laboratory, Cold Spring Harbor, NY
15 Bers, D., Patton, C. and Nuccitelli, R. (1994) Methods Cell Biol. **40**, 3–29
16 Brooks, S. P. J. and Storey, K. B. (1992) Anal. Biochem. **201**, 119–126
17 Walker, C. J. and Willows, R. D. (1997) Biochem. J. **327**, 321–333
18 Thorneley, R. N. F. and Lowe, D. J. (1983) Biochem. J. **215**, 393–403
19 Thorneley, R. N. F. (1992) Phil. Trans. R. Soc. Lond. B **336**, 73–82
20 Walker, J. E., Saraste, M., Runswick, M. J. and Gay, N. J. (1982) EMBO J. **1**, 945–951
21 Chin, D. T., Goff, S. A., Webster, T., Smith, T. and Goldberg, A. (1988) J. Biol. Chem. **263**, 11718–11728
22 Jakob, U., Scheibel, T., Bose, S., Reinstein, J. and Buchner, J. (1996) J. Biol. Chem. **271**, 10035–10041
23 Ryle, M. J. and Seefeldt, L. C. (1996) Biochemistry **35**, 4766–4775
24 Lanzilotta, W. N., Fisher, K. and Seefeldt, L. C. (1996) Biochemistry **35**, 7188–7196
25 Lanzilotta, W. N., Fisher, K. and Seefeldt, L. C. (1997) J. Biol. Chem. **272**, 4157–4165
26 Huang, H.-W. and Cowan, J. A. (1994) Eur. J. Biochem. **219**, 253–260
27 Buchler, J. W. (1975) in Porphyrins and Metalloporphyrins (Smith, K., ed.), pp. 157–232, Elsevier, Amsterdam
28 Kini, R. M. and Evans, H. J. (1995) Biochem. Biophys. Res. Commun. **212**, 1115–1124
29 Gibson, L. C. D., Marrison, J. L., Leech, R. M., Jensen, P. E., Bassham, D. C., Gibson, M. and Hunter, C. N. (1996) Plant Physiol. **111**, 61–71
30 Walker, C. J. and Weinstein, J. D. (1991) Proc. Natl. Acad. Sci. U.S.A. **88**, 5789–5793
31 Stanier, R. Y. and Cohen-Bazire, G. (1977) Annu. Rev. Microbiol. **31**, 225–274
32 Richter, M. L. and Rienits, K. G. (1982) Biochim. Biophys. Acta **717**, 255–264
33 Dailey, H. A. (1982) J. Biol. Chem. **257**, 14714–14718
34 Matringe, M., Camadro, J.-M, Joyard, J. and Douce, R. (1994) J. Biol. Chem. **269**, 15010–15015

Received 1 April 1998/2 June 1998; accepted 19 June 1998